

UCSB Astro Journal Club

John McCann

13 November 2015

Astrophysical calibration of gravitational-wave detectors

M. Pitkin,^{1,*} C. Messenger,^{1,†} and L. Wright^{1,‡}

¹*SUPA, School of Physics and Astronomy, University of Glasgow, Glasgow G12 8QQ, United Kingdom*

(Dated: November 10, 2015)

We investigate a method to assess the validity of gravitational-wave detector calibration through the use of gamma-ray bursts as standard sirens. Such signals, as measured via gravitational-wave observations, provide an estimated luminosity distance that is subject to uncertainties in the calibration of the data. If a host galaxy is identified for a given source then its redshift can be combined with current knowledge of the cosmological parameters yielding the true luminosity distance. This will then allow a direct comparison with the estimated value and can validate the accuracy of the original calibration. We use simulations of individual detectable gravitational-wave signals from binary neutron star (BNS) or neutron star-black hole (NSBH) systems, which we assume to be found in coincidence with short gamma-ray bursts, to estimate any discrepancy in the overall scaling of the calibration for detectors in the Advanced LIGO and Advanced Virgo network. We find that the amplitude scaling of the calibration for the LIGO instruments could on average be confirmed to within $\sim 10\%$ for a BNS source within 100 Mpc. This result is largely independent of the current detector calibration method and gives an uncertainty that is competitive with that expected in the current calibration procedure. Confirmation of the calibration accuracy to within $\sim 20\%$ can be found with BNS sources out to ~ 500 Mpc.

Sections

- I. Introduction
- II. Gravitational wave detector calibration
- III. Binary neutron star standard sirens
- IV. GRB counterparts
- V. Analysis
 - a. Method
 - i. Prior ranges
 - b. Simulations
- VI. Results
 - 1..1 Parameter biases
- VII. Discussion

Objects of Interest[†]

- Strongest candidates for first gravitational wave detections are from compact binary coalescences (CBCs)
- Mean estimates of future CBC detections are $O(10)$ per year
 - Binary neutron star (BNS) mergers out to ~ 450 Mpc ($z \approx 0.1$)
 - Neutron star-black hole systems
- CBCs are also likely sources of short gamma ray burst (sGRB)
 - Inferred rates of sGRB CBC events: $8 \times 10^{-9} - 1.1 \times 10^{-6} \text{ Mpc}^{-3} \text{ yr}^{-1}$
 - For reference BNS merger rates: $10^{-8} - 10^{-5} \text{ Mpc}^{-3} \text{ yr}^{-1}$
NSBH merger rates: $6 \times 10^{-10} - 10^{-6} \text{ Mpc}^{-3} \text{ yr}^{-1}$
- CBCs are natural “standard sirens,” moreover directly observing a sGRB can also tell us the distance—**two independent measures for calibration**

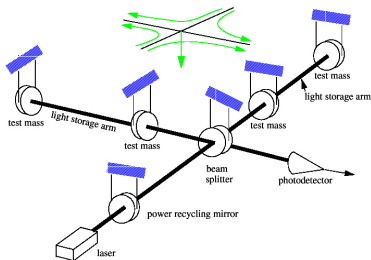
[†]All estimates here taken from paper

Detection methods for gravitational waves (GW)

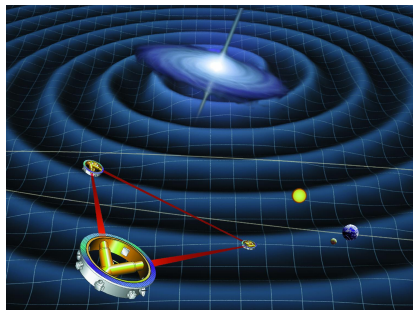
- “Popular” methods of detection
 - Laser interferometers
 - Resonant mass detectors
 - Pulsar timing
 - Spacecraft tracking
 - Cosmic microwave background temperature perturbations
- These methods are not exactly redundant as different methods are better at probing different frequencies of gravitational waves —think EM spectrum

Interferometers

- aLIGO, [a]VIRGO, GEO600, [KAGRA], [LIGO-India], [eLISA]
- LIGO & VIRGO: Michelson interferometers with Fabry-Perot cavities



(a) Schematic of LIGO/VIRGO



(b) eLISA

Existing GW detector calibration

- GW strain is measured through ΔL , i.e., $h(f, t) = \Delta L(f, t)/L$
- Need to calibrate measured signal $e(f, t)$ to actual ΔL , via $\Delta L(f, t) = R(f)e(f, t)$, for some response function $R(f)$
- You measure $R(f)$ through measurements in feedback loop, but feedback is off by some C , which you wish to calibrate.

$$Ch_{true}(f) = h_m(f) = \frac{R(f)e(f)}{L}. \quad (1)$$

- $C > 1$ implies overestimating signal, source appears closer, and opposite for $C < 1$
- Current methods get the error in C to within $\sim 10\%$

Propagation of gravitational waves

- Weak field Einstein equation in vacuum reduces to 3D wave equation

$$(-\partial_t^2 + \nabla^2)\bar{h}^{ab} = 0 \rightarrow \bar{h}^{ab} = A^{ab} \exp[ik_c x^c]. \quad (2)$$

- In transverse-traceless gauge: $\bar{h}_{ab}^{TT} = h_{ab}^{TT}$ (traceless condition)

$$\bar{h}^{ab}{}_{,b} = 0; \quad A^a{}_a = 0; \quad A_{ab}U^b = 0. \quad (3)$$

- Moreover, only two independent constants, A_{xx}^{TT} and A_{xy}^{TT} . Traceless implies $A_{xx}^{TT} = -A_{yy}^{TT}$ and $A_{xy}^{TT} = A_{yx}^{TT}$ from symmetric metric, rest zero by gauge choice.

Geodesic deviation

- In frame of test particle geodesic deviation equation to first order in perturbing metric (R vanishes in flat space) becomes

$$\partial_t^2 \xi^a = -R^a{}_{0b0} \xi^b. \quad (4)$$

- Since we only consider first order perturbations Riemann components are

$$R^x{}_{0x0} = -\frac{1}{2} \partial_t^2 h_{xx}^{TT}; \quad R^y{}_{0x0} = -\frac{1}{2} \partial_t^2 h_{xy}^{TT}; \quad R^y{}_{0y0} = -\frac{1}{2} \partial_t^2 h_{yy}^{TT}. \quad (5)$$

- Consider particle distance ϵ from test particle in x direction

$$\partial_t^2 \xi^x = \frac{1}{2} \epsilon \partial_t^2 h_{xx}^{TT}; \quad \partial_t^2 \xi^y = \frac{1}{2} \epsilon \partial_t^2 h_{xy}^{TT}. \quad (6)$$

- Now ϵ in y direction

$$\partial_t^2 \xi^x = \frac{1}{2} \epsilon \partial_t^2 h_{xy}^{TT}; \quad \partial_t^2 \xi^y = \frac{1}{2} \epsilon \partial_t^2 h_{yy}^{TT} = -\frac{1}{2} \epsilon \partial_t^2 h_{xx}^{TT}. \quad (7)$$

Gravitational wave polarizations

- From our geodesic deviation we see there are two polarizations:
 $h_{xx} \neq 0, h_{xy} = 0$ denoted '+' and $h_{xy} \neq 0, h_{xx} = 0$ denoted 'x'

(c) Plus GW polarization

(d) Cross GW polarization

- For binary systems: $h_+ \propto (1 + \cos^2(\theta))$ and $h_x \propto \cos(\theta)$

Generating gravitational waves[†]

- Weak field Einstein equation in region of source

$$(-\partial_t^2 + \nabla^2)\bar{h}_{ab} = -16\pi T_{ab}. \quad (8)$$

- Assumptions: $T_{ab} = S_{ab}(x^i)e^{i\Omega t}$ and source region $\ll \frac{2\pi}{\Omega}$
- Then a possible solution is of the form

$$\bar{h}_{ab} = B_{ab}(x^i)e^{i\Omega t}. \quad (9)$$

- Consider $(\nabla^2 + \Omega^2)B_{ab} = -16\pi S_{ab}$ outside the source ($S_{ab} = 0$)

$$B_{ab} = \frac{A_{ab}}{r}e^{i\Omega r} + \frac{Z_{ab}}{r}e^{-i\Omega r}. \quad (10)$$

- Only using outgoing waves, $Z_{ab} = 0$.

[†]I'll neglect retarded time effects for simplicity

- To solve for A_{ab} integrate

$$\int (\nabla^2 + \Omega^2) B_{ab} d^3x = \int -16\pi S_{ab} d^3x. \quad (11)$$

- Recall source is confined to region ϵ , so first term

$$\int \Omega^2 B_{ab} d^3x \leq \Omega^2 |B_{ab}|_{\max} 4\pi\epsilon^3/3. \quad (12)$$

- Second term by Gauss's theorem and having solution outside source

$$\int \nabla \cdot \nabla B_{ab} d^3x = \oint \vec{n} \cdot \nabla B_{ab} dS = 4\pi\epsilon^2 \left(\frac{d}{dr} B_{ab} \right)_{r=\epsilon}. \quad (13)$$

- Putting it all together[†]

$$\Omega^2 |B_{ab}|_{\max} 4\pi\epsilon^3/3 - 4\pi A_{ab} [1 + \Omega^2\epsilon^2/2 - i\Omega\epsilon^3/3] = -16\pi J_{ab}. \quad (14)$$

- Now using the approximation that $\Omega\epsilon \ll 2\pi$

$$A_{ab} = 4J_{ab} \rightarrow \bar{h}_{ab} = 4J_{ab} e^{i\Omega(r-t)}/r. \quad (15)$$

[†] $\int S_{ab} d^3x = J_{ab}$

- By stress-energy conservation and Gauss's theorem

$$i\Omega J^{\mu 0} e^{-i\Omega t} = \int T^{\mu j}{}_{;j} d^3x = \oint T^{\mu j} n_j dS = 0. \quad (16)$$

- Thus $\bar{h}_{\mu 0} = 0$, for spatial components use tensor virial theorem

$$\partial_t^2 \int T^{00} x^i x^j d^3x = 2 \int T^{ij} d^3x; \quad I^{jk} \equiv \int T^{00} x^i x^j d^3x. \quad (17)$$

- Therefore the spatial components of J_{ij}

$$J_{ij} = \frac{1}{2} \partial_t^2 (D_{ij} e^{-i\Omega t}) e^{i\Omega t} = -\frac{\Omega^2}{2} D_{ij}. \quad (18)$$

- This is known as the quadrupole approximation for gravitational radiation

$$\bar{h}_{ab} = -2\Omega^2 D_{ab} e^{i\Omega(r-t)}/r. \quad (19)$$

Quadrupole perturbing metric

- Since we have used the slow motion approximation ($\Omega\epsilon \ll 2\pi$), then $T^{00} \approx \rho$, thus I_{ij} looks like the moment of inertia tensor
- In TT gauge[†]

$$\bar{h}_{xx}^{TT} = -\bar{h}_{yy}^{TT} = -\Omega^2(I_{xx} - I_{yy})e^{i\Omega r}/r. \quad (20)$$

$$\bar{h}_{xy}^{TT} = -2\Omega^2 I_{xy} e^{i\Omega r}/r. \quad (21)$$

- Recall TT gauge implies gravitational wave is propagating in the z-direction

[†] $I_{ab} \equiv I_{ab} - \frac{1}{2}\delta_{ab}I^c_c$

Gravitational waves from binary systems

- Consider an idealized circular binary system with masses m_1 and m_2

$$x_1(t) = \frac{\mu}{m_1} a \cos(\omega t); \quad y_1(t) = \frac{\mu}{m_1} a \sin(\omega t). \quad (22)$$

$$x_2(t) = \frac{-\mu}{m_2} a \cos(\omega t); \quad y_2(t) = \frac{-\mu}{m_2} a \sin(\omega t). \quad (23)$$

- Wave eq. is linear, and we want $-i\Omega t$ solutions we get

$$\bar{h}_{xx}^{TT} = -a^2 \Omega^2 \mu e^{i\Omega r - 2i\omega t} / r \rightarrow \bar{h}_{xx}^{TT} = -4a^2 \omega^2 \mu e^{i\Omega(r-t)} / r. \quad (24)$$

$$\bar{h}_{xy}^{TT} = -ia^2 \Omega^2 \mu e^{i\Omega r - 2i\omega t} / r \rightarrow \bar{h}_{xy}^{TT} = -4ia^2 \omega^2 \mu e^{i\Omega(r-t)} / r. \quad (25)$$

- We note that radiation frequency is twice orbital ($\Omega = 2\omega$)

Gravitational waves from binary systems: II

- To look at radiation coming from the x -direction redo calculations with $(x, y, z) \rightarrow (y, z, x)$
- You get no '×' polarization because masses stay in plane, by same logic '+' polarization is halved

$$\bar{h}_{yy}^{TT} = -\bar{h}_{zz}^{TT} = 2a^2\omega^2\mu e^{i\Omega(r-t)}/r. \quad (26)$$

- All perturbations are of order $a^2\omega^2\mu/r \rightarrow Gm_1m_2/(ar)$. This is why we can hope to detect these but not the Newtonian tidal forces
- Best realistic case: formation of $10M_\odot$ black hole, in nearby universe $\rightarrow O(h) = 10^{-18}$
- Norm: PSR B1913+16[†], $m_1 = m_2 = 1.4M_\odot$, $a = 8.37 \times 10^{12}$ m, $r = 8$ kpc $\rightarrow O(h) = 10^{-23}$

[†]Really $O(h) = 10^{-26}$; but $O(h) = 10^{-20}$ systems believed

Gravitational waves as a standard siren

From the quadrupole approximation for gravitational radiation[†]

$$\langle h \rangle = 10^{-23} m_T^{2/3} \mu f_{100}^{2/3} r_{100}^{-1}. \quad (27)$$

$$\tau = \frac{f}{\dot{f}} = 7.8 m_T^{-2/3} \mu^{-1} f_{100}^{-8/3} \text{ s}. \quad (28)$$

Solving for $m_T^{2/3} \mu$ in both equations, equating and solving for r_{100} results in

$$r_{100} = 7.8 f_{100}^{-2} (\langle h_{23} \rangle \tau)^{-1}. \quad (29)$$

The RHS is completely determined by observations, allowing for a “standard siren” to measure distances free of the cosmic ladder.

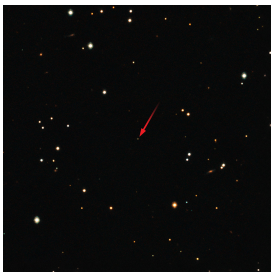
[†] $r_{100} \equiv r/100 \text{ Mpc}$; $f_{100} \equiv f/100 \text{ Hz}$; $h_{23} = h \times 10^{23}$

Backing out variables from observations

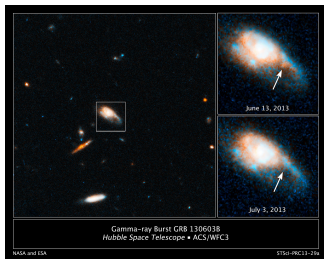
- Note that $\langle h \rangle$ is the r.m.s. value, but observed value will depend on binary orientation to detector
- Given 3 detectors possible to determine orientation of binary
 - Time delay of incoming GW at θ to connecting line: $\Delta t = d \cos(\theta)/c$
 - Generally polarization will be out of phase between detectors
 - Five unknowns: arrival direction (2), polarization amplitudes (2), phase lag of polarization (1)
 - Knowns: time delays ($n - 1$ independent), measured amplitudes (n)
 - To determine system: $n + (n - 1) \geq 5$, so $n \geq 3$ —overdetermining system helps beats down error in r_{100}
- Backing out direction determines orientation, thus $\langle h \rangle$
- f_{100} and τ can be directly observed, completely determining r_{100}

sGRB

- GRB are associated with the most powerful known events
- GRB cause the region to light-up at various wavelengths—afterglow
- Due to relativity beams are highly collimated, thus detections are rare
- sGRB are classified as a GRB with a duration less than 2 seconds



(e) ESO followup Swift's 1000 GRB



(f) kilonova afterglow

Joint CBC–sGRB detections

- 0.2–200 BNS events/year
- 1–180 sGRB/year[†]
- 0.02–7 joint detections/year
- They will be detecting GW and do followup for sGRB afterglow
- Likelihood of catching concurrent sGRB from GW detection: “low”[‡]
- Possible observe sGRB and look for GW event[§]
 - Less computationally expensive, fewer number of waveform templates
 - Enables multi-detector coherent schemes, better than coincidence
- Overall, joint-detections allow for orientation to be a known, from sGRB beaming angle, allowing for higher signal to noise

[†] Assuming 15° collimation

[‡] “Compounded” with GW error box of ~ 100 's square degrees

[§] Swift already great at relaying GRB information fast

Goal

Assess how well calibration scale factor can be estimated from single GW–sGRB co-detection. We'll want to be at least competitive with current methods of $\sim 10\%$.

Measured data

- LIGO's polarization model, our naive work was of close order, given by

$$\tilde{h}_+(f) \propto (1 + \cos^2(i)) D_L^{-1} \mathcal{M}^{5/6} f^{-7/6} e^{-i\Psi(f, \mathcal{M}, t_c, \phi_c)}. \quad (30)$$

$$\tilde{h}_\times(f) \propto \cos^2(i) D_L^{-1} \mathcal{M}^{5/6} f^{-7/6} e^{-i\Psi(f, \mathcal{M}, t_c, \phi_c)}. \quad (31)$$

- Fourier transform of GW strain at k -th detector, with antenna response functions F —dependent on polarization angle and sky position

$$\tilde{h}^k(f) = F_+^k(\alpha, \delta, \psi) \tilde{h}_+(f) + F_\times^k(\alpha, \delta, \psi) \tilde{h}_\times(f). \quad (32)$$

- Measured data, with true noise \tilde{n} and waveform parameters θ , then given by

$$\tilde{d}_k(f) = C_k(\tilde{n}_k(f) + \tilde{h}_k(f, \theta)) \quad (33)$$

The likelihood function[‡]

- Adopt a Gaussian likelihood function

$$\mathcal{L}(\boldsymbol{\theta}, \mathbf{C}, I | \mathbf{d}) = p(\mathbf{d} | \boldsymbol{\theta}, \mathbf{C}, I) \propto \exp \left[-4\Delta f \sum_{k=1}^{N_{\text{det}}} \sum_{i=i_{\text{low}}}^{i_{\text{high}}} \frac{|d_{k,i} - C_k \tilde{h}_{k,i}|^2}{S_{k,i}} \right]. \quad (34)$$

- S is the noise power spectrum distribution, and $I = \{i_{\text{low}}, \dots, i_{\text{high}}\}$ [†]
 - Analyzed frequency range is 20—400 Hz, $\sim 95\%$ of BNS events

[†]I presume...

[‡]They claim to use “Bayes’ theorem”

Prior PDFs

- Events that are co-detected give us more information on the priors
 - Analysis uses sGRB to say source distance is δ -function prior
 - Moreover, sky position also a δ -function prior
 - Events also relatively face-on, so nearly circularly polarized
- sGRB beaming poorly understood, adopt half-normal distribution with median of $\iota = 10^\circ \rightarrow$ prior ι is Gaussian with $\sigma = 14.8^\circ$
- Prior on masses[†] assumed Gaussian
 - BNS: $\mu = 1.35 M_\odot$, $\sigma = 0.13 M_\odot$
 - NSHB: $\mu = 5 M_\odot$, $\sigma = 1 M_\odot$
- Several other priors are left as uniform: time of coalescence, t_c (± 0.01 s about recorded), reference phase, ϕ_c , polarization angle, ψ

[†]Constrained from an observation—prior not too important 

Prior PDF on calibration scale factor

- Use log-normal distribution, peaked near 1 and probability of calibration being either too small by 'x' or too big by 'x' are equal

$$p(C|I) = \frac{1}{C\sigma\sqrt{2\pi}} \exp\left[-\frac{(\log(C) - \mu)^2}{2\sigma^2}\right]. \quad (35)$$

- $\sigma = 1.07$ and $\mu = 1.15$, “arbitrarily” chosen $\sigma \rightarrow \mu = \sigma^2$ (mode at 1)
 - Arbitrarily: $P(C = 10)/P(C = 1) \approx P(C = 1/10)/P(C = 1) \approx 1/10$
 - Log-normal also favors close to above unity, over close to below unity

BNS & NSBH simulated events

- Now need to simulate data, which will
- Simulations of BNS and NSBH signals spanning 20–400 Hz
 - BNS range from 50–500 Mpc at 50 Mpc increments
 - BHNS range from 100–900 Mpc at 100 Mpc increments
 - $O(1000)$ simulations at each distance, randomly drawing from prior distribution and randomly throughout the sky (uniform)
- Criteria for detection $\text{SNR} \geq 5.5$ in at least two detectors
 - Leading to a selection of effect of face-on (circularly polarized)
 - Also preferred sky locations at large distances (best antenna response)

Figures 1 & 2

- Three detectors used in these simulations: two aLIGO (H1 and L1) and the AdV (V1)
- Posterior distributions have been generated from the likelihood and priors via simulations
- Give minimal 68% credible region for calibration factors
- Figure 1 for BNS systems and Figure 2 for NSBH systems at selected distances

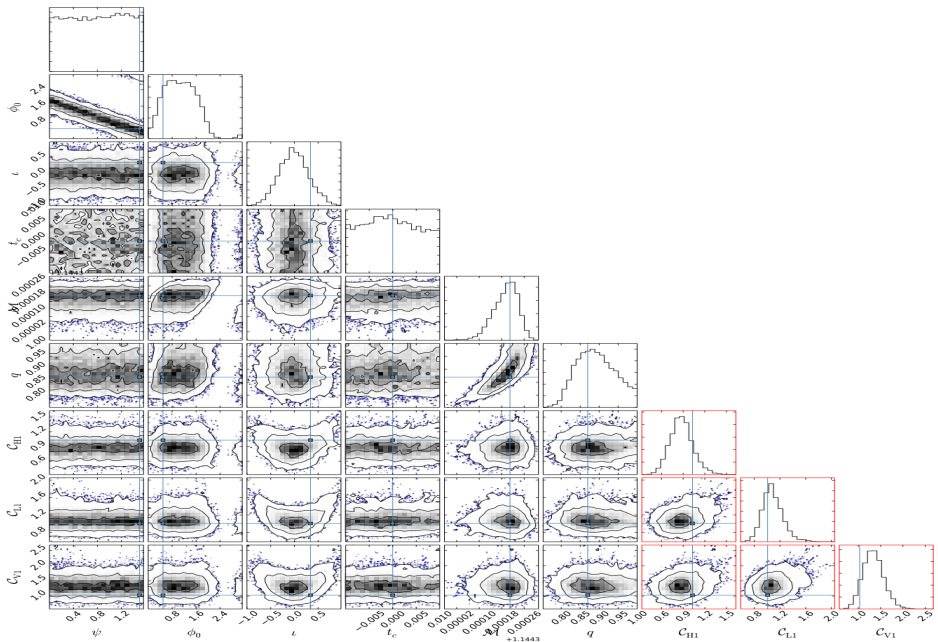


FIG. 1: The marginalised posterior probability distributions for the unknown parameters of a BNS system, including calibration scaling factors (surrounded by the red borders) for the three detectors (H1, L1 and V1). The simulated signal was at a distance of 250 Mpc, had SNR of 8.7, 10.9 and 4.1 and percentage relative uncertainties in the calibration scale factors of 14%, 11% and 27% for each of the detectors respectively.

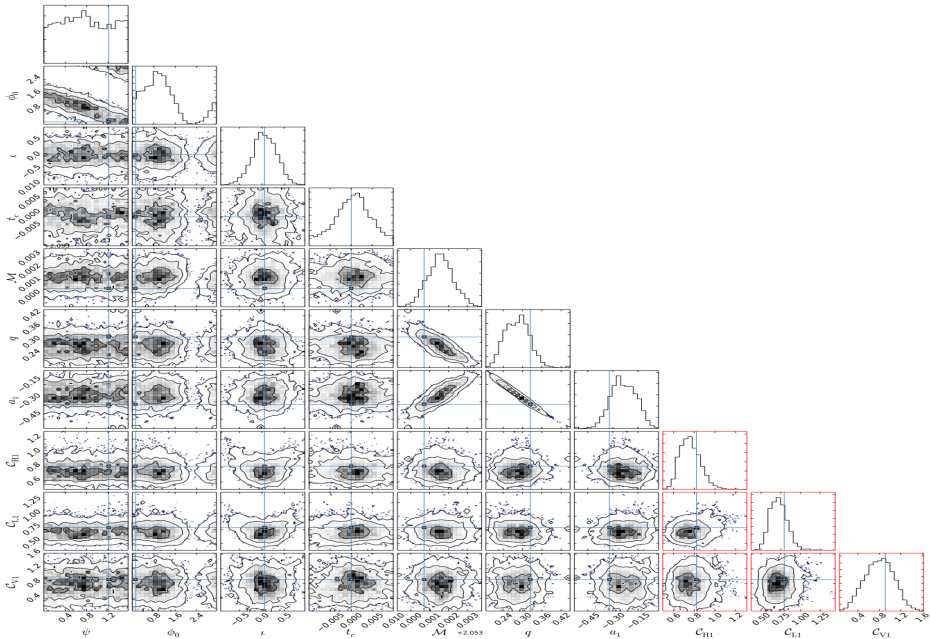


FIG. 2: The marginalised posterior probability distributions for the unknown parameters of a NSBH system, including calibration scaling factors for the three detectors (H1, L1 and V1). The simulated signal was at a distance of 450 Mpc, had SNR of 7.7, 10.9 and 4.2 and percentage relative uncertainties in the calibration scale factors of 17%, 14% and 34% for each of the detectors respectively.

Figures 3 & 4

- From posterior distributions, calculated at each distance is: σ (box bars), 2σ (whiskers), median (black line), mean (star), and percentage of signals fulfilling SNR criterion (dashed magenta line)

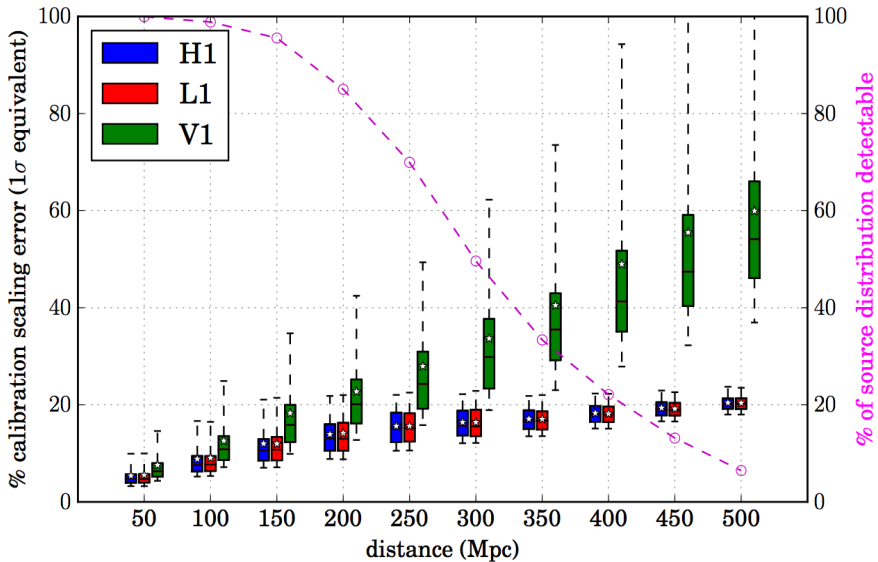


FIG. 3: Distributions of the percentage accuracy at which the calibration scale factors can be determined for a three detector network if using BNS systems (provided a coincident GRB is observed and can yield a distance estimate). The boxplots span the lower to upper quartile range of the distributions, with the median value shown as a horizontal line within the box and the mean shown as a white star. The dashed magenta line shows the percentage of sources drawn from the prior distribution that would be detectable at each distance value.

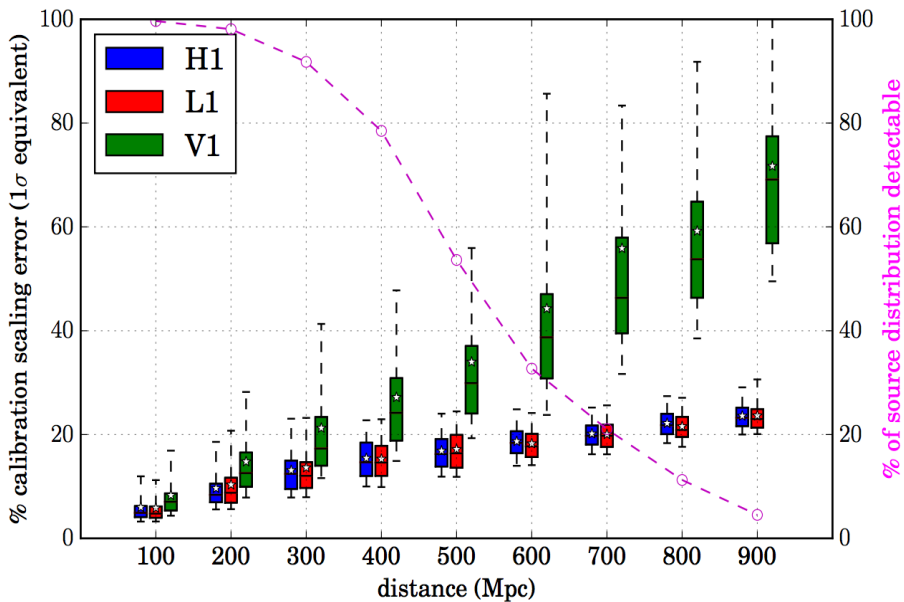
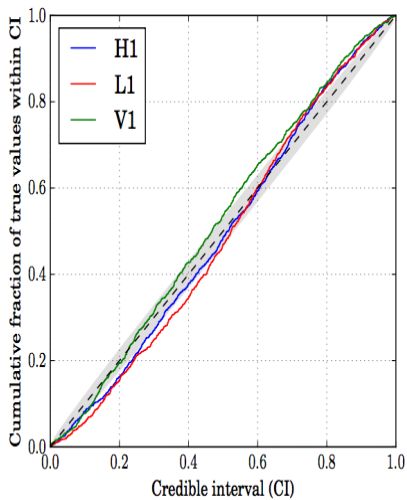


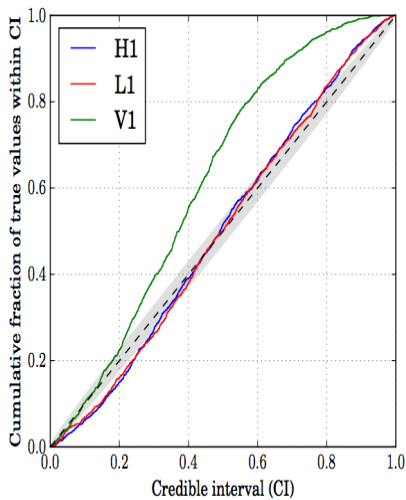
FIG. 4: Distributions of the percentage accuracy at which the calibration scale factors can be determined for a three detector network if using NSBH systems (provided a coincident GRB is observed and can yield a distance estimate). The plot contents are the same as in figure 3.

Figure 5

- Calculate self-consistency of PDFs at 50 & 500 Mpc for BNS
- Closer to the diagonal the better



(a)



(b)

FIG. 5: Both figures shows the cumulative fraction of true \mathcal{C} values found within a given fractional credible interval versus fractional credible interval for each detector for the BNS simulations at (a) 50 Mpc and (b) 500 Mpc. The grey shaded region is a 95% credible band for the expected deviations from diagonal.

Discussion

- For BNS calibration scale factor on average within
 - 10% out to 100 Mpc
 - 20% out to 450 Mpc
- Similar results for NSBH
- Significant delay between observation and calibration assessment
 - However, gives independent check
- Possible for relative calibration between detectors
 - They'd like a continuous GW source for this though
 - This would help account for sky location biases for burst sources (CBC)